Real-Time Monitoring of Fluorescence Anisotropy and Temperature During Processing of Biaxially Stretched Polypropylene Film[1]

ANTHONY J. BUR* *and* STEVEN C. ROTH

Polymers Division
National Institute of Standards and Technology
Gaithersburg, MD 20899-8542

An optical sensor based on fiber optics has been developed to measure fluorescence anisotropy and temperature during processing of biaxially stretched polypropylene films. The sensor, containing optical fibers, polarizing elements and lenses, was mounted above the polypropylene film as it was processed in a tenter frame oven stretching machine. Fluorescence observations were made using the fluorescent dye, bis (di-tert butylphenyl) perylenedicarboximide (BTBP), which was doped into the resin at very low concentrations. To monitor biaxial stretching, fluorescence anisotropy measurements were carried out with light polarized in the machine and the transverse directions corresponding to the directions of biaxial stretching. Fluorescence based temperature measurements were obtained from the ratio of fluorescence intensities at 544 nm and 577 nm. A matrix of experiments involving three levels of stretch ratio in both the machine and transverse directions was undertaken. We observed significant differences between anisotropy in the machine and transverse directions that we attributed to the sequential stretching operation, i.e., the film was stretched in the machine direction first, followed by stretching in the transverse direction, and to film temperature and strain rate for each stretching operation. The result was uniformly higher anisotropies in the machine direction. Film temperature obtained from fluorescence corresponded to oven thermocouple measurements within 2°C. Polym. Eng. Sci. 44:805–813, 2004.

INTRODUCTION

Biaxially stretched polyolefin films are used extensively in packaging applications. For food packaging in particular, barrier properties for oxygen and water vapor are critical for maintaining shelf life, and mechanical and thermal properties are important for product preparation that involves wrapping and heat sealing. The properties and performance of the film are determined by the molecular orientation that is created in the film by applied extensional stresses. The most efficient method of manufacturing biaxially oriented polypropylene (BOPP) film is continuous processing that involves stretching in a tenter frame at elevated temperatures. Machine parameters that can be adjusted to control molecular orientation are stretch ratios, strain rates, and temperature. The most common industrial practice involves a sequential operation in which an extruded polymer sheet is stretched in the machine (MD) direction followed by stretching in the transverse direction (TD).

Very little technical information about tenter frame biaxial stretching processes has been published. Recently, Wilkes and co-workers discussed the tenter processing of high density polyethylene (HDPE), but their publication contained abbreviated results as they discussed only half of the operation, namely MD stretching and microstructure characterization of the HDPE film after MD stretch (1). Because their process was carried out sequentially, MD stretching followed by TD stretch, the information that they obtained provided the basis from which TD stretch was undertaken, but no post TD stretch data were presented. MD stretching experiments were carried out as a function of stretch

[1]This work was performed under a Cooperative Research and Development Agreement (CRADA) between NIST and Collaborator ExxonMobil Chemical Co. Under the terms of the CRADA, this document may not be used as advertising for any product or service, nor may Collaborator imply to anyone that the CRADA or the research results are an endorsement by NIST of any Collaborator products or services.
*To whom correspondence should be addressed. E-mail: abur@nist.gov

Published online in Wiley InterScience (www.interscience.wiley.com).
DOI 10.1002/pen.20072

ratio and stretch temperature, after which they examined the state of HDPE film by various off-line techniques including X-ray, atomic force microscopy (AFM), transmission electron microscopy, and differential scanning calorimetry, and refractive index observations. Their examination focused on the change in crystalline morphology from spherulitic lamellae into lamellar stacks that resulted from MD stretch at temperatures near the melting temperature. In another study, Nie and co-workers used AFM after BOPP processing to examine surface properties, but a detailed examination of the biaxial stretching process was not carried out (2).

Laboratory methods to characterize molecular orientation of the film product, such as X-ray diffraction, AFM, and birefringence, are usually carried out in post-processing tests, and many off-line experimental studies of biaxial orientation and microstructure in blown film and uniaxial orientation of crystalline polymers have been published (3–10). But there have been very few approaches to microstructure studies using on-line techniques. An on-line measurement of birefringence was developed by Cakmak and co-workers and was used to monitor uniaxial stretching of polyethylene naphthalate (11, 12). The technique revealed gross orientation as well as subtle changes and the evolution of new microstructure during annealing. A method for on-line continuous monitoring of molecular orientation is desirable because it can yield a database record of the process, can be utilized immediately to adjust machine parameters to make a desired product, and can be used as a sentry to detect quality problems. In this paper, we report the development and implementation of an on-line, real-time sensor based on fluorescence spectroscopy to monitor both orientation and temperature of biaxially stretched polypropylene. While X-ray and birefringence measurements exclusively reflect or are dominated by crystalline orientation, a fluorescence anisotropy measurement of a fluorescent dye that has been added to the resin should primarily reflect amorphous orientation, which has a more profound effect on the marginal improvement or variation of film properties.

The sensor combines two process monitoring concepts, temperature and anisotropy, that we have developed during the past several years using fluorescence techniques (13–15). The measurement relies on the presence of a fluorescent dye that is mixed with the resin at low concentrations, less than 10^{-5} mass fraction of dye in the resin. The dye used for this work is bis (di-tert butylphenyl) perylenedicarboximide (BTBP), a dye that possesses large molecular geometrical anisotropy. BTBP is called a band definition dye and belongs to a class of dyes whose spectra show marked temperature dependence (14). The large geometrical anisotropy enhances its orientation in extensional flows. Its size precludes inclusion in the crystalline structure of polypropylene (PP). The molecular structure of BTBP is shown in *Fig. 1*, where the double-headed arrow is the direction of the absorption dipole.

Fluorescence anisotropy measurements yield information about the orientation of the absorption dipole moment of a fluorescent dye that has been excited with polarized light. The technique has been used to measure molecular orientation in polymer melts and in solid polymer films and fibers (15–22). Orientation information is obtained from the polarization of the emitted fluorescent light. For this application, the direction of the incident light is polarized alternately in the machine direction (MD) and the transverse direction (TD). We measure two anisotropies, r_M and r_T, corresponding to excitation light polarized in the machine and transverse directions:

$$r_M = \frac{I_{MM} - I_{MT}}{I_{MM} + 2I_{MT}} \qquad r_T = \frac{I_{TT} - I_{TM}}{I_{TT} + 2I_{TM}} \tag{1}$$

where I_{MM} and I_{MT} are, respectively, the intensities of fluorescent light polarized in the machine and transverse directions, produced by incident light polarized in the machine direction, and I_{TT} and I_{TM} are, respectively, the intensities of fluorescent light polarized in the transverse and machine directions, produced by incident light polarized in the transverse direction. *Equation 1* expresses anisotropy as the difference between intensities of mutually perpendicular polarizations of fluorescence divided by the approximate total

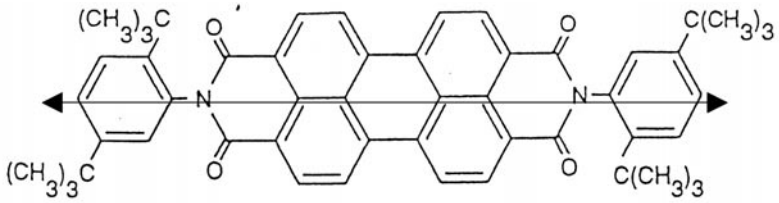

bis(-di-tert-butylphenyl)-perylenedicarboximide

(BTBP)

Fig. 1. The molecular structure of BTBP. The arrow is in the direction of the absorption dipole.

fluorescence intensity. Anisotropy r is a dimensionless quantity, theoretically limited to the range -0.5 to $+1$ and independent of the amount of dye.

Several authors have developed molecular models that yield a relationship between r and absorption dipole orientation factors (17, 19, 21, 23, 24). These theoretical models are not employed in this study. Instead, we take the approach that an empirical application of *Eq 1* can yield qualitative and operational principles regarding the biaxial film stretching process. If temperature is held constant during an experiment, it is possible to obtain a set of internally consistent data that reveal the effects of orientation. The data presented below were obtained at constant temperature and pressure so that the observed changes in anisotropy are due to molecular orientation as expressed in the geometrical orientation factors of the dye's absorption dipole moment.

According *Eq 1*, the measurement of r_M and r_T involves the separate observations of pairs of fluorescence intensities, I_{MM} and I_{MT}, and I_{TT} and I_{TM}. For online, real-time observations, each pair of intensities must be measured simultaneously. The sensor that we employ here is designed to detect the pair intensities simultaneously, and we will demonstrate its use for monitoring r_M and r_T during biaxial stretching of polypropylene film in a tenter oven at approximately 160°C. We present the results from real-time process monitoring carried out at different machine set-points.

The second function of the sensor, to monitor temperature, is based on the shape of the fluorescence spectrum and its dependence on temperature. The technique has been described in detail in previous publications (13, 14). Briefly, the ratio of intensities at two wavelengths vs. temperature is the basis for obtaining the temperature of the resin in the dye's molecular neighborhood. The calibration procedure is discussed in the next section.

EXPERIMENTAL PROCEDURE[2]

Our experiments were conducted on a Marshall and Williams tenter frame biaxial stretching machine at the pilot plant facility of ExxonMobil Chemical Co. in Macedon, N.Y. In the tenter frame stretching operation, polypropylene resin is first extruded into a strip or sheet that is cooled below its crystallization temperature. After traversing a series of rollers as it crystallizes and anneals, the strip is brought to the entrance of the oven, where it is grabbed at both edges by moving clamps of the tenter frame and pulled into the oven (1). The entry zones of the tenter frame oven were maintained at 132°C. For our experiments, stretching was carried out sequentially, first MD and followed by TD stretching. Typical conditions for MD stretching were 132°C at 13 s^{-1} strain rate, and for TD stretching they were 158°C at 0.6 s^{-1}, declining to 0.075 s^{-1} over the length of the stretch zone. After MD and TD stretching, the film was pulled through the annealing section of the oven set at 160°C where the anisotropy sensor was positioned. The MD and TD mechanical stretch ratios, s_M and s_T, were varied systematically to study the relationship between fluorescence anisotropy and process parameters. r_{MD} and r_{TD} were measured at all nine combinations of s_M = 4, 5, 6 and s_T = 6.6, 8, 10 by holding s_T constant while increasing s_M in steps to 4, 5 and 6. For each set of eighteen measurements, the anisotropy sensor was moved along a positioning rail to three positions on the transverse axis, designated as West, Central and East, where the Central position was at the center of the film and East and West were separated from it by 0.46 m. The full set of measurements yielded 54 data points. Since winding speed and tenter stretch zone length were kept constant, changes in stretch ratio were accompanied by proportionate changes in strain rate.

Fluorescence Anisotropy Sensor (15). A sketch of the sensor is shown in *Fig. 2*. The stainless steel sensor head has a rectangular cross section (38.1 mm by 50.8 mm) in order to maintain a recognizable direction of light polarization. The solid stainless steel block (106 mm length) has been machined with channels and compartments that receive the optical fibers and optical components, and it is blackened in order to reduce internal light reflections. Focusing and polarizing optics, needed to excite a fluorescent dye with polarized light and to analyze the polarization of the generated fluorescence, are placed in internal compartments that secure their position when the sensor is in operation. Excitation light at 488 nm, produced by an air-cooled argon ion laser from Coherent, is transmitted to the sensor and specimen via one or the other of the optical fibers positioned in the sensor channels. Light polarized in the **machine** direction is produced when light travels along the center channel path and directly through the calcite crystal. Light polarized in the **transverse** direction is produced by light that travels the side channel path. The fiber-optic bundles in both channels of the sensor head are bifurcated into two branches, with one branch transmitting excitation light and the other collecting and carrying fluorescence to the detector. Both fiber cables have identical design consisting of nineteen 200 μm core fused silica fibers, eighteen of which carry fluorescence to the detector, and the other single fiber transmits the excitation light. One central fiber for excitation light is surrounded by eighteen fibers for fluorescence collection. A single excitation fiber was deemed necessary because a uniform focus of light onto the PP film is best produced by a single fiber rather than several fibers. The total length of the fiber cable is 4 m with bifurcated branches having 0.5 m length. The fiber bundle is protected over the length of the cable with stainless steel strip wound flexible sheathing. Fiber cables of our custom design were purchased from Schott-Fostec. More detail about polarization optics, light paths, and sensor construction is available in Reference 15.

[2]Identification of a commercial product is made only to facilitate experimental reproducibility and to describe adequately the experimental procedure. In no case does it imply endorsement by NIST or imply that it is necessarily the best product for the experiment.

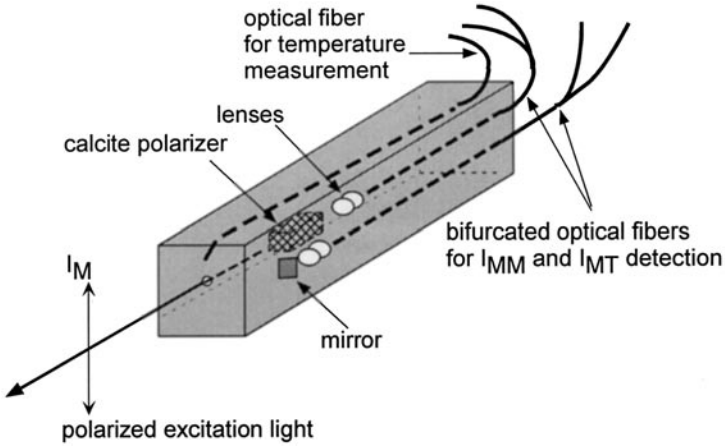

Fig. 2. A drawing of the sensor head with optical fibers.

A block diagram of the full setup is shown in *Fig. 3*. The entire optics assembly was placed in a light-tight enclosure in order to eliminate stray light from entering the photomultiplier tubes (PMTs). A beamsplitter divides the excitation light at 488 nm from the laser into two beams directed to optical fibers in the center and side channels of the sensor. Shutters open to direct the laser beam to these channels one at a time, and alternately open and close at 10 s intervals. The generated fluorescence, which has transmitted through the calcite crystal polarizer and is collected by optical fibers in the center and side channels, corresponds to light polarized in the machine and transverse directions respectively. Each intensity measurement was a photon count integrated over 1 s. Ten such measurements of I_{MM} and I_{MT} were taken simultaneously; then the shutters were switched to repeat the procedure for I_{TT} and I_{TM}. This sequence was repeated 10 to 20 times in a row, after which the TD sensor position was changed. The r data reported below are therefore based on averages of 100 to 200 intensity measurements. r_M and r_T are not measured simultaneously, but this is of little consequence because we observed the steady state condition of the process over an extended period of time, 15 min or more at each machine set-point.

Detection of fluorescence is done with photomultiplier tubes and Stanford Research SR400 photon counter. At the entrance to each PMT, light passes through a dispersion prism that deflects 488 nm excitation light away from the PMT, but fluorescence with $\lambda > 500$ nm passes through wide-band filters transmitting over the most intense part of the fluorescence spectrum, 510 nm to 590 nm.

In order to account for the difference between fluorescent light transmission through the side and center channels, calibration of the sensor is necessary. This

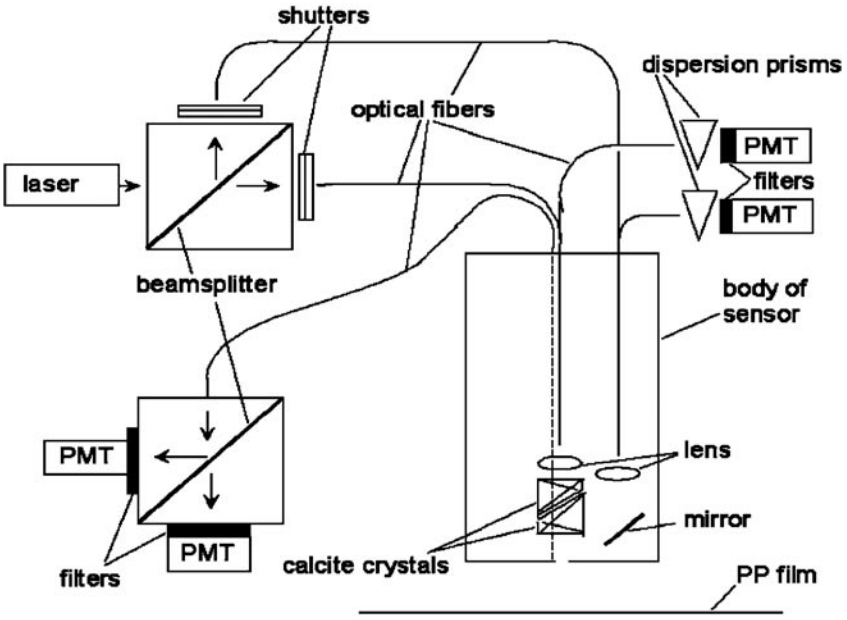

Fig. 3. A block diagram of the entire experimental up.

involves obtaining a value for g, the ratio of transmissions in the two branches. The calibration consists of measuring r_M and r_T of an oriented film at room temperature, then rotating the film 90° and repeating the measurements to obtain r'_M and r'_T. At 0° the expressions for r containing the g-factor are

$$r_M = \frac{I_{MM} - gI_{MT}}{I_{MM} + 2gI_{MT}} \qquad r_T = \frac{gI_{TT} - I_{TM}}{gI_{TT} + 2I_{TM}} \tag{2}$$

At 90° we have

$$r'_M = \frac{I_{MM} - gI_{MT}}{I_{MM} + 2gI_{MT}} \qquad r'_T = \frac{gI_{TT} - I_{TM}}{gI_{TT} + 2I_{TM}} \tag{3}$$

The equivalence between the 0° and 90° measurements dictates that

$$r'_M = r_T \qquad r'_T = r_M \tag{4}$$

These two equations provide two independent values of g, which should be close to each other if experimental error is low. The g-factors determined following this procedure were found to be $g = 0.318$ and $g' = 0.337$. This discrepancy is small compared to the precision required here. The root mean square relative error is minimized for $g = 0.327$.

The third channel in the sensor contains collection optical fibers that transmit fluorescence to the PMT detectors for the temperature measurements. This is shown as the dashed line in the sensor body of *Fig. 2*. These fibers collect fluorescence and direct it to a beamsplitter that separates the fluorescence into two beams that are filtered respectively at the 544 nm and 577 nm with narrow bandpass filters positioned at the entrance to the detecting PMTs. Photons from the PMTs are counted using another SR400 photon counter, and the ratio I_{544}/I_{577} is used to calculate the temperature from the calibration curve of *Fig. 4*. The fluorescence temperature was calibrated by slowly raising the oven temperature from about 70°C to about 150°C and then lowering it back to 70°C with a stationary piece of BOPP film. The ratio $\beta = I_{544}/I_{577}$ and air temperature T of the BOPP film were measured simultaneously where T was obtained from a thermocouple touching the film near the focused excitation light beam. The increasing and decreasing temperature data are very well fitted by distinct straight lines, which differ slightly (3%) in slope. The difference can be entirely explained by the air-film thermal lag. Taking the averages of slopes and intercepts produces an accurate calibration equation.

The sensor was located in the annealing section of the oven 15 mm above the film surface and immediately after MD and TD stretching had occurred. Thus, we were not observing the dynamics of the stretching operation, but the post stretching and annealed condition of the film. The sensor could be placed in any TD position by means of a traversing mechanism. Measurements were taken at the tenter centerline and near the West and East film edges as depicted in *Fig. 5*. The TD dimension of the film, which depended on the stretch ratio, was approximately 1.5 m. By means of the traversing rail, the sensor could be raised and shuttled to a background measurement station where anisotropy readings were taken at process temperature against a non-fluorescent, non-reflective black surface. A background measurement series preceded each West-Center-East fluorescence measurement sequence. Background intensities I^b_{MM}, I^b_{MT}, I^b_{TT} and I^b_{TM} were obtained and subtracted from the corresponding intensities measured later on oriented film.

The biaxially stretched film material is made from polypropylene doped with BTBP dye. The polypropylene was Fina 3371. BTBP was purchased from Aldrich

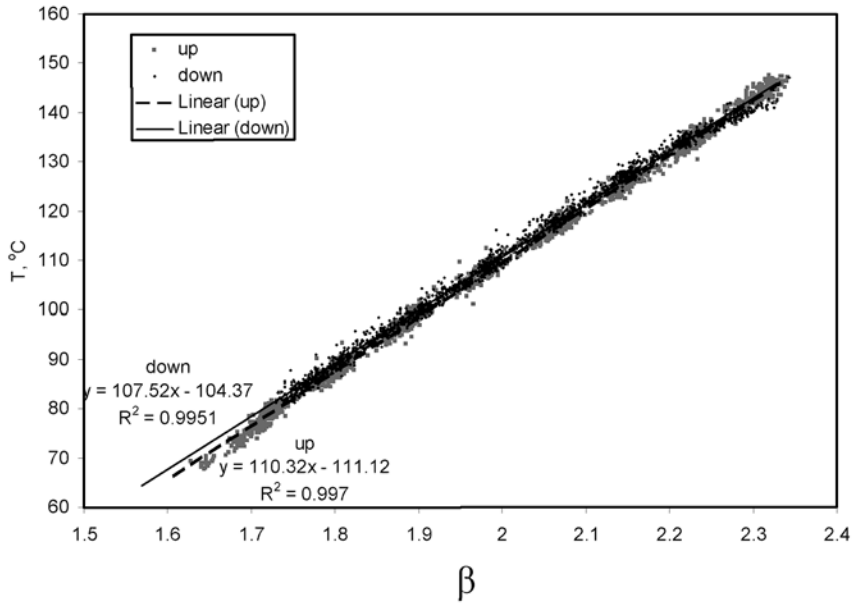

Fig. 4. Temperature versus the ratio of fluorescence intensity at 544 nm and 577 nm. $\beta = I_{544}/I_{577}$.

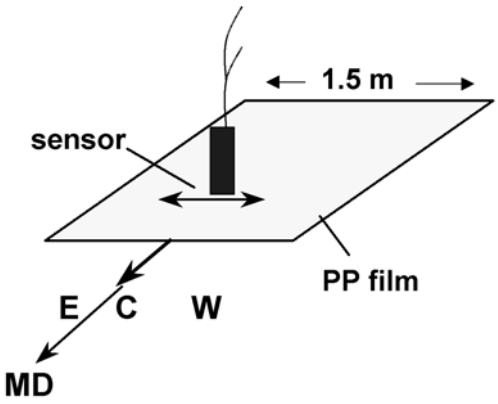

Fig. 5. A drawing showing the position of the sensor and the East, Center, and West positions.

Chemical Co. Doping of the dye into the polypropylene resin was carried out by pouring a solution of BTBP dye in toluene over resin pellets, followed by evaporation of the solvent, leaving behind pellets coated with BTBP. These pellets and additional neat polymer were then passed through a twin-screw extruder at 200°C and repelletized. The final concentration of dye in the resin is 6.6×10^{-6} mass fraction. Film thickness was 25 μm. Note that concentration uniformity of the dye and thickness uniformity of the film are not essential since the *r*'s (*Eq 1*) and β are normalized.

RESULTS AND DISCUSSION

Figure 6 shows typical results of the fluorescence temperature measurement along with readings from a thermocouple that was positioned in the air 12 mm away from the film. Data were obtained for the steady state process. Surprisingly good agreement between thermocouple and fluorescence data is observed, allowing for air-film thermal lag. The data show that the temperature of the film was maintained between 155°C and 162°C in the annealing section of the oven where the oven set temperature was 160°C.

The bar charts of *Fig. 7* summarize r_{MD} and r_{TD} measurements obtained at West, Central and East positions. The dominant feature of these data is that the machine direction anisotropy was almost always higher than transverse anisotropy. This is attributed to the three factors: the sequence of stretching, first in the machine direction followed by transverse stretching, the temperature of the film at each stretching zone, and the strain rate of each stretch. As mentioned above, typical conditions for MD stretching were 132°C at 13 s^{-1} strain rate, and for transverse direction stretching they were 158°C at 0.6 s^{-1}, declining to 0.075 s^{-1} over the length of the stretch zone. The lower temperature of machine extension accompanied by the relatively high strain rate favored larger MD molecular orientation compared to TD. Also, the transverse stresses were applied to a film that was already oriented in the machine direction so that transverse orientation stress works against an established orthogonal orientation, whereas machine direction stretch was imposed upon a randomly oriented strip of polypropylene. Transverse stretching was carried out at relatively low strain rates in order to maintain the integrity of the film, and the result is low molecular orientation in that direction compared to the machine direction.

The standard deviation of *r* can be estimated from the variances and covariances of the I^b_{kl} and I_{kl}'s through a first order Taylor series approximation to *r* derived from *Eq 1* (25). Note that each I_{kl} in this equation is a *net* intensity, so $I_{kl} - I^b_{kl}$ should be substituted for I_{kl}.

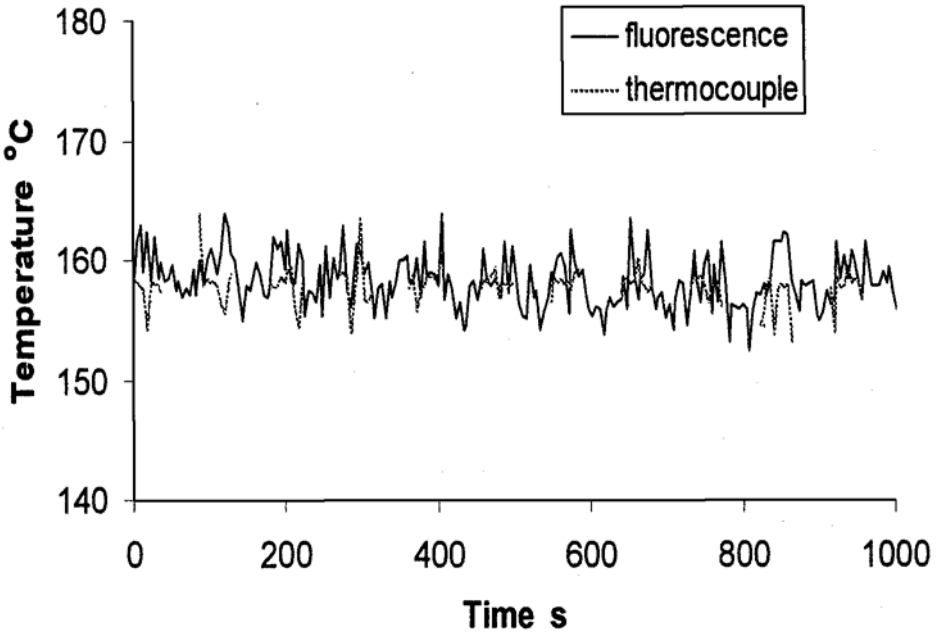

Fig. 6. Real-time measurement of temperature from fluorescence and the thermocouple.

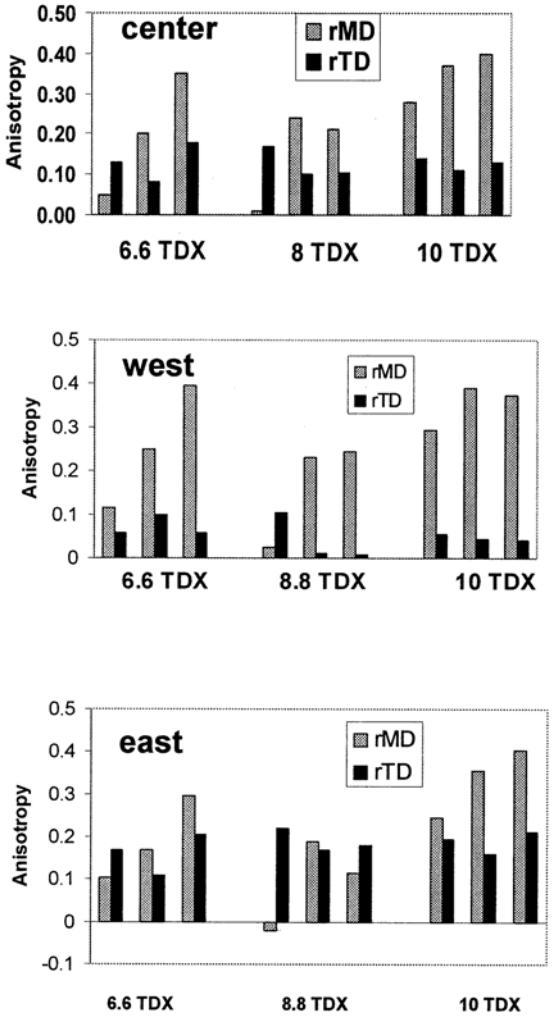

Fig. 7. Bar charts of r_M and r_T at the East, Center, and West positions.

The indirect approximate calculation method is necessitated by the fact that I_{kl} and I^b_{kl} values are not paired. For all cases tested, we found standard deviation of r_T between 0.006 and 0.008. The standard deviation of r_M was larger, ranging from 0.03 to 0.07. However, even this is not a concern, since the relevant quantity is the standard uncertainty of the mean, which is smaller than the standard deviation by a factor $\sqrt{n}$, where n = number of data values, which was greater than 100 here.

Three near-zero values of r_{MD} for MDX = 4 and TDX = 8 at East, Central and West positions appear to be an anomaly when compared to the remaining set of data. Were these data obtained from the same experimental run, they would be treated as outliers. However, the three data points were obtained from three separate runs, all of which had different background intensities that were used to obtain the measured anisotropy values. Although the cause of the low r_{MD} values is not known, these observations reveal new information about the process and the range of r_{MD} values that result from an array of processing conditions.

The data from the eighteen anisotropy measurements obtained at the Center position are shown in *Figs. 8* and *9*. In *Fig. 8*, r_M is plotted against s_M, with s_T as parameter, since intuitively, s_M should be the primary determinant of r_M. Indeed, r_M generally increases with s_M. Less obvious is the fact that r_M also increases to a lesser extent with s_T. This can be attributed to the fact that TD stretch contributes to r_M by reducing out-of-plane molecular orientation.

A multiple regression using data from the Center position yields

$$r_M = -0.790 + 0.118 s_M + 0.0544 s_T \quad (R^2 = 0.772) \quad (5)$$

The statistical significance of both coefficients is very high, and potential second or higher-order terms are

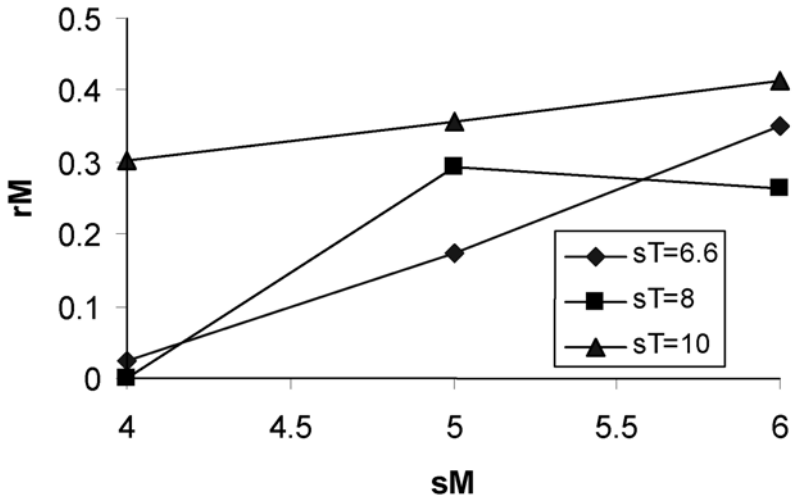

Fig. 8. Anisotropy r_M as a function of MD stretch ratio at various TD stretch ratios. Data are from Center position.

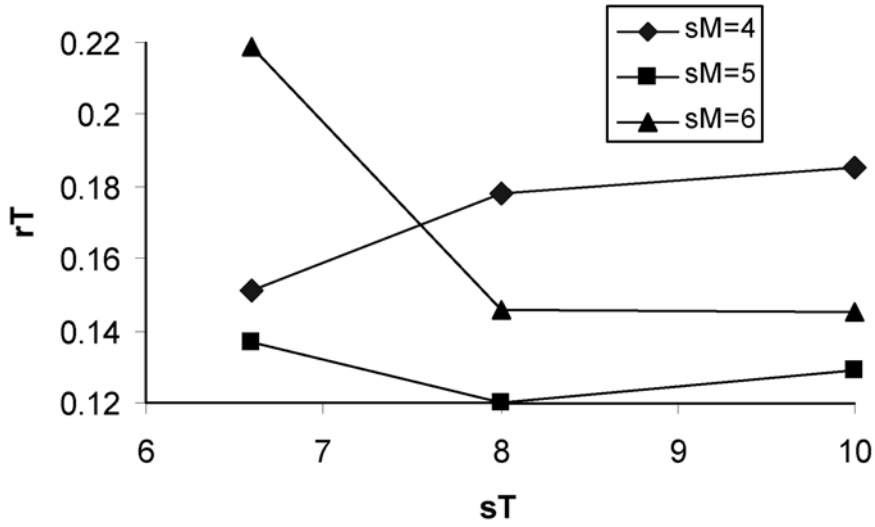

Fig. 9. Anisotropy r_T as a function of TD stretch ratio at various MD stretch ratios. Data are from Center position.

not significant. The standard uncertainty of fit is 0.08. Whether this moderate lack of fit is due to experimental uncertainty or to other factors controlling orientation is unknown. However, crystallinity plays no role because the dye is present in the amorphous phase only. Multiple regression using the full set of r_M data from East, Center and West positions yields the following:

$$r_M = -0.582 + 0.0925 s_M + 0.0431 s_T \quad R^2 = 0.602 \quad (6)$$

A similar attempt to fit the r_T data using multiple regressions yielded statistically insignificant relationships for all sensor positions. The value of r_T is not influenced by machine direction stretching, and, as seen in *Fig. 7*, transverse stretching beyond 6.6 had little effect on r_T. The data of *Fig. 9* show that r_T does not monotonically increase with s_T or s_M. Part of the difficulty may be due to the smaller range of r_T compared to r_M. This can be seen more clearly in *Fig. 10*, which includes data from all TD positions. Another important conclusion from this figure is the absence of correlation between r_M and r_T. Hence, these two orientation indices are independent. This is not surprising in a biaxially orientated film, which requires two orientation factors for complete characterization.

In *Fig. 10*, also note the systematic difference in r_T between the East, Center and West positions. In fact, this difference is comparable in magnitude to some of the effects in *Fig. 8*. In other words, film of varying effective stretch ratio was produced at different TD positions. Yet the film made throughout these experiments had less than 3% gauge variation and no visual defects. This exemplifies the hidden non-uniformities this method can help detect.

CONCLUSIONS

The satisfactory operation of the fluorescence temperature and anisotropy sensor was demonstrated during biaxial stretching of polypropylene film in a tenter oven. The two anisotropy measures r_T and r_M were

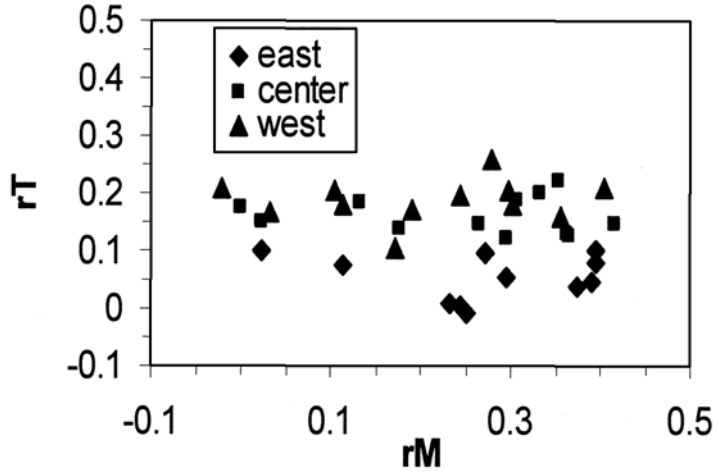

Fig. 10. r_T versus r_M for all stretch ratio experiments and all three positions.

consistent with each other as shown by the g-factor calibration. The r measurements for the biaxially stretched polypropylene film were also statistically independent of each other. The standard uncertainties of the anisotropy measurements were low. At steady state, web temperature measured by fluorescence agreed well with adjacent air temperature measured by thermocouple.

In a designed experiment carried out with the instrument in a tenter oven, r_M followed intuitive expectations in its dependence on the MD and TD stretch ratios. The behavior of r_T could not be explained easily, but the low strain rates and relatively high temperature of the TD stretch are most likely the basis for the r_T observations. Significant TD positional variation in r_T was detected on the particular tenter used.

ACKNOWLEDGMENTS

The authors wish to acknowledge a very fruitful collaboration with Moris Amon of ExxonMobil Chemical Co., who assisted us while installing the anisotropy sensor and running the experiments on the ExxonMobil tenter frame oven process line.

REFERENCES

1. V. Ratta, G. L. Wilkes, and T. K. Su, *Polymer,* **42**, 9059 (2001).
2. H. Y. Nie, M. J. Walzak, and N. S. McIntyre, *Polymer,* **41**, 2213 (2000).
3. H. Y. Zhou and G. L. Wilkes, *J. Mater. Sci.,* **33**, 287 (1998).
4. R. J. Pazur and R. E. Prud'homme, *Macromol.,* **29**, 119 (1996).
5. T. C. Ma and C. D. Han, *J. Appl. Polym. Sci.,* **35**, 1725 (1988).
6. Y. M. Kim, C. H. Kim, J. K. Park, C. W. Lee, and T. I. Min, *J. Appl. Polym. Sci.,* **63**, 289 (1997).
7. A. Perterlin, *Colloid Polym. Sci.,* **253**, 809 (1975).
8. I. L. Hay and A. Keller, *J. Mater. Sci.,* **4**, 908 (1969).
9. R. J. Samuels, *Structured Polymer Properties,* John Wiley, New York (1974).
10. P. B. Bowden and R. J. Young, *J. Mater. Sci.,* **9**, 2034 (1974).
11. J. Galay and M. Cakmak, *J. Polym. Sci. Polym. Phys.,* **39**, 1107 (2001).
12. J. Galay and M. Cakmak, *J. Polym. Sci. Polym. Phys.,* **39**, 1147 (2001).
13. A. J. Bur, M. G. Vangel, and S. C. Roth, *Polym. Eng. Sci.,* **41**, 1380 (2001).
14. A. J. Bur, M. G. Vangel, and S. C. Roth, *Appl. Spec.,* **56**, 174 (2002).
15. A. J. Bur, S. C. Roth, and C. L. Thomas, *Rev. Sci. Instr.,* **71**, 1516 (2000).
16. Y. Nishio, H. Suzuki, and K. Sato, *Polymer,* **35**, 1452–1461 (1994).
17. A. J. Bur, C. L. Thomas, S. C. Roth, and F. W. Wang, *Macromol.,* **25**, 3503 (1992).
18. B. Erman and L. Monnerie, *Polymer,* **28**, 727 (1987).
19. J. H. Nobbs, D. I. Bower, I. M. Ward, and D. Patterson, *Polymer,* **15**, 287 (1974).
20. L. L. Chappoy, K. Rasmussen, and D. B. DuPre, *Macromol.,* **20**, 680 (1979).
21. P. Lappersonne, P. Sergot, L. Monnerie, and G. LeBourvellec, *Polymer,* **30**, 1558 (1989).
22. S. Maruse, M. Hirami, Y. Nishioi, and M. Yamamoto, *Polymer,* **38**, 4577 (1997).
23. A. Szabo, *J. Chem. Phys.,* **72**, 4620 (1980).
24. C. Zannoni, *Mol. Phys.,* **38**, 1813 (1979).
25. A. Hald, *Statistical Theory With Engineering Applications,* John Wiley, New York (1952).